Open Access Online Journal on Astronomy and Astrophysics

Acta Astrophysica Taurica

www.astrophysicatauricum.org

Acta Astrophys. Tau. 5(2), 13–16 (2024)

Precursors of solar flares in the microwave range

V.E. Abramov-Maximov[1], I.A. Bakunina[2]

[1] Central (Pulkovo) Astronomical Observatory of RAS, Pulkovskoye sh. 65/1, St. Petersburg 196140, Russia
e-mail: beam@gaoran.ru
[2] HSE University, Bolshaya Pecherskaya 25/12, Nizhny Novgorod 603155, Russia

Received 31 October 2021

ABSTRACT

We present a study of the spatial distribution of quasiperiodic oscillations of microwave emission in two active regions before M-class flares. We have studied two events: NOAA 11283 on September 6 and NOAA 11302 on September 25, 2011. We used the Nobeyama Radioheliograph (NoRH) daily observations at a frequency of 17 GHz. In both cases we found the preflare wave trains of brightness temperature oscillations of microwave emission in active regions. The duration of wave trains is about 3–4 oscillation cycles. We found that the source of oscillations was a compact zone in the active region, which coincides with the area of maximum brightness during a flare.

Key words: Sun, flares, radio emission, quasiperiodic oscillations

1 Introduction

Quasiperiodic oscillations (QPOs) of microwave emission from solar active regions (ARs) were discovered about 50 years ago (Durasova et al., 1971). Indications of a correlation between QPO parameters and flare activity were obtained almost immediately (Kobrin et al., 1973a, b; Aleshin et al., 1973; Korshunov, Prokof'eva, 1976). Independently, different authors detected an effect of power enhancement of QPO microwave emission directly before a flare (Berulis et al., 1973; Arbuzov, 1979; Kobrin et al., 1981; Aver'yanikhina et al., 1982; Berulis et al., 1983; Avdyushin et al., 1985). Moreover, a similar effect of enhancement in geomagnetic field pulsations before proton flares was detected, as well as its relation to solar radio emission pulsations (Bystrov et al., 1978, 1979).

However, the capabilities of instruments in the 70s–80s were quite limited. A significant advancement in QPO studies in the microwave range occurred thanks to the operation of the Nobeyama Radioheliograph (NoRH) (Gelfreikh et al., 1999, 2006). Continuous solar observations were carried out with NoRH from 1992 to 2020 for 7–8 hours daily with a time resolution of 1 s in the standard mode at frequencies of 17 and 34 GHz, registering intensity (Stokes parameter I) and circular polarization (Stokes parameter V, only at 17 GHz). The angular resolution is 10–20″ at a frequency of 17 GHz, which allows distinguishing individual components of radio emission in ARs. Using the observational data from NoRH, several cases of increased QPO power were detected before flares with periods ranging from 3 to 100 minutes (Sych et al., 2009; Abramov-Maximov et al., 2011; Abramov-Maximov, Bakunina, 2018, 2019, 2020). A similar enhancement effect of QPOs before flares was detected in soft X-ray emission according to GOES data (Tan et al., 2016).

During a flare, a significant restructuring of the magnetic field in the AR occurs, and consequently, a sharp change in plasma parameters, which likely leads to modifications in the observed characteristics of QPOs. This can be used for coronal plasma diagnostics. On the one hand, analyzing the preflare QPOs of AR emission could help in advancing our understanding of the processes occurring during the development of a flare, and on the other hand, possibly in developing new short-term criteria for the forecast of geoeffective flares.

This work aims to study the spatial distribution of QPOs observed before flares in active regions.

2 Observations

2.1 Used observational data and processing method

Observations of the Sun were conducted using NoRH at a frequency of 17 GHz (1.76 cm) in intensity (Stokes parameter I). We investigated the spatial distribution of microwave emission for two active regions: NOAA 11283 and 11302, observed on September 6 and 25, 2011, respectively.

Table 1 provides information on the flares that occurred in the considered ARs during the observation interval using NoRH, according to the Space Weather Prediction Center's Preliminary Report and Forecast (SWPC PRF) No. 1880 and 1882[1]. It is essential for our work that there were no other

[1] ftp://ftp.ngdc.noaa.gov/STP/swpc_products/weekly_reports/PRFs_of_SGD/

Table 1. Data on the flares on September 6 and 25, 2011 within the NoRH observation time interval according to SWPC PRF bulletins No. 1880 and 1882. Column "Start" shows the onset of flares; "Peak", the maximum of flares; "Stop", the ending of flares; GOES, the power of flares according to the GOES classification.

NOAA	Date	Start	Peak	Stop	GOES
11283	September 6, 2011	01:35	01:50	02:05	M5.3
11302	September 25, 2011	02:27	02:33	02:37	M4.4
11302	September 25, 2011	03:27	03:32	03:38	C7.9
11302	September 25, 2011	04:31	04:50	05:05	M7.4

flares before the M5.3 flare on September 6 and the M4.4 flare on September 25 from the beginning of observations with NoRH, which allows using these intervals for detecting QPOs.

For the analysis of QPOs in NOAA AR 11283, the ready-made images in fits format with a 3-minute cadence were used[2]. For the analysis of QPOs in NOAA AR 11302, the synthesis of radio images was performed in the nonstandard mode with a cadence of 1 minute and averaging time of 10 seconds according to the Koshix algorithm. Then for both ARs, the studied AR (field-of-view – FOV) was highlighted on all full-disk solar images, taking into account the rotation of the Sun, and the time profiles of brightness temperatures in six selected pixels of the AR image were constructed.

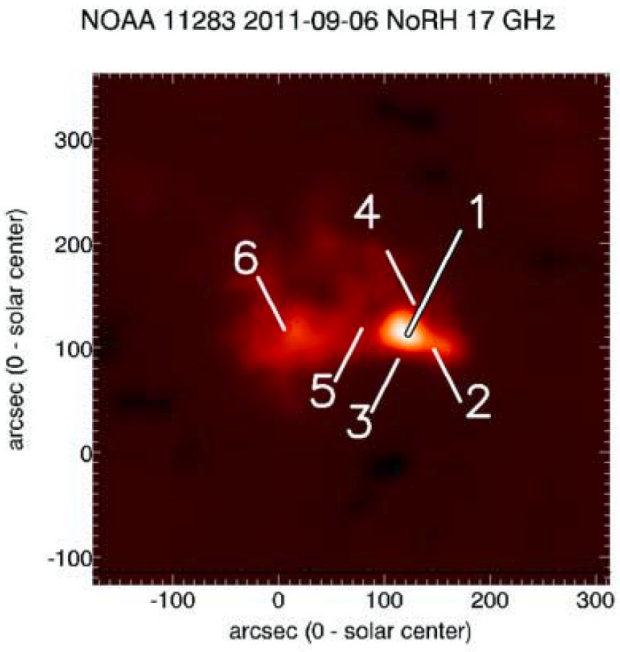

Fig. 1. Image of NOAA AR 11283 from observations with the Nobeyama Radioheliograph on September 6, 2011 at a frequency of 17 GHz in intensity (Stokes parameter I). We indicate the positions of pixels in the AR image for which radio emission time profiles shown in Fig. 2 are constructed.

[2] https://solar.nro.nao.ac.jp/norh/fits/3min/

A fragment of the solar radio image at a frequency of 17 GHz containing NOAA AR 11283 is presented in Fig. 1, outlining the positions of the pixels for which time profiles of brightness temperatures have been constructed. A similar fragment for NOAA AR 11302 is shown in Fig. 3. The corresponding time profiles of brightness temperatures at a frequency of 17 GHz are shown in Figs. 2 and 4. Let us consider them in more detail.

2.2 Preflare time profiles of microwave emission from NOAA AR 11283

Figure 2 shows the fragments of the time profiles highlighted in red from the beginning of observations to the start of the M5.3 class flare. The same fragments are displayed separately in red insets at the same scale.

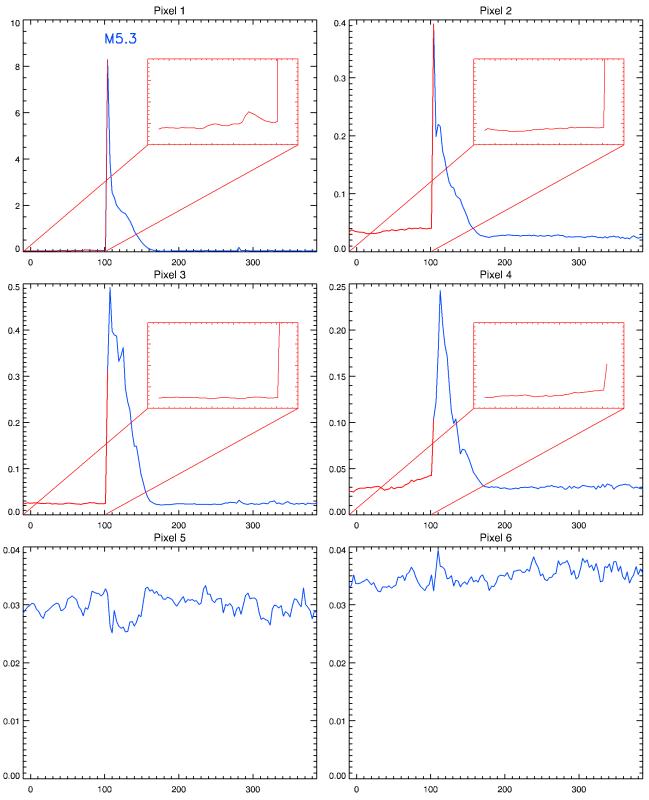

Fig. 2. Time profiles of microwave emission from different areas of NOAA AR 11283 (pixel positions are indicated in Fig. 1) at a frequency of 17 GHz in intensity (Stokes parameter I) from observations with the Nobeyama Radioheliograph on September 6, 2011. The preflare sites are shown in red in time profiles 1–4. The preflare fragments of time profiles are shown on an enlarged scale in the red insets. The scale is the same in all red insets. In all panels, along the abscissa – time in minutes since the beginning of the UT day (0 corresponds to 00:00 UT); along the ordinate – brightness temperature in MK.

Figure 2 shows that in pixel 5, which corresponds to the interspot area, and in pixel 6, located in the trailing spot, there are no changes in the character of the time profiles throughout the entire day of observation. Pixel 1 is located in the leading spot and area in which the maximum brightness temperature

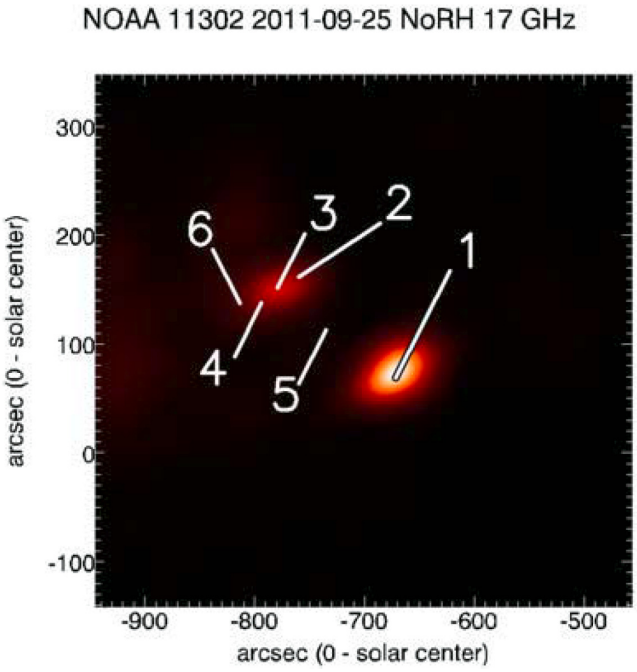

Fig. 3. Image of NOAA AR 11302 from observations with the Nobeyama Radioheliograph on September 25, 2011 at a frequency of 17 GHz in intensity (Stokes parameter I). We indicate the positions of pixels in the AR image for which radio emission time profiles shown in Fig. 4 are constructed.

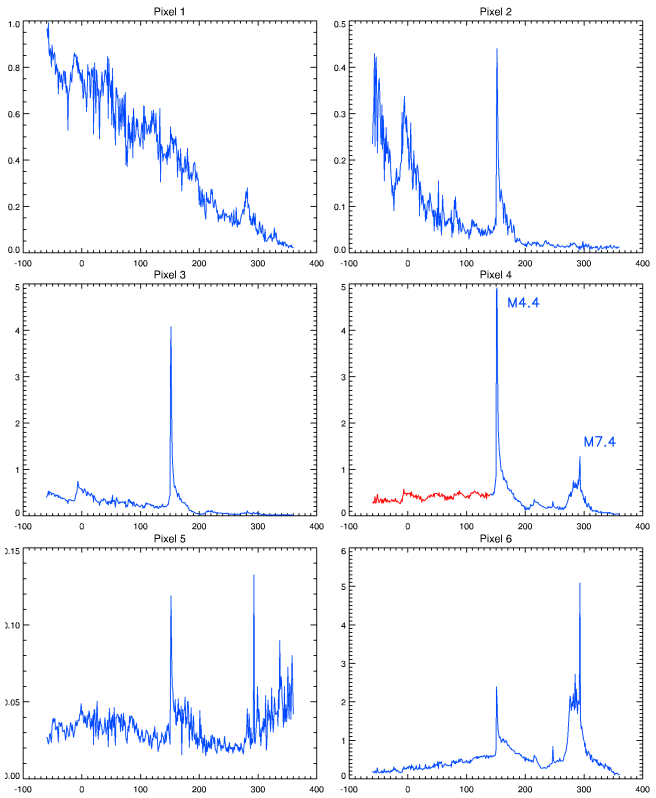

Fig. 4. Time profiles of microwave emission from different areas of NOAA AR 11302 (pixel positions are indicated in Fig. 3) at a frequency of 17 GHz in intensity (Stokes parameter I) from observations with the Nobeyama Radioheliograph on September 25, 2011. The preflare wave train is shown in red in the time profile for pixel 4. In all panels, along the abscissa – time in minutes since the beginning of the UT day (0 corresponds to 00:00 UT), along the ordinate – brightness temperature in MK.

was observed during the flare. It is precisely in this pixel that a preflare wave train with a duration of about 60 minutes, consisting of 3 oscillation cycles, is evident. It should be noted that in all previously detected preflare wave trains with completely different durations (from several minutes to an hour or more), the number of oscillation cycles was no more than 10 and amounted on average to 5 (Abramov-Maximov, Bakunina, 2020).

Pixels 2, 3, and 4 correspond to the periphery of the leading spot. A flare in the microwave range is observed in them but an order of magnitude weaker than that in pixel 1. In pixel 3, only a weak hint at QPOs can be noticed, and in pixels 2 and 4, QPOs are not visible.

Thus, in NOAA AR 11283 on September 6, 2011, a preflare wave train of QPOs of the brightness temperature of microwave emission is observed, which is generated in the same compact zone over the leading spot of the AR where the maximum brightness temperature was recorded during the flare.

2.3 Preflare time profiles of microwave emission from NOAA AR 11302

Figure 4 shows that in pixel 1, which corresponds to the leading spot, neither the flare nor oscillations manifest themselves. In pixels 2, 3, 5, and 6, the flare is visible to some extent, but no significant oscillations are seen. The most pronounced preflare wave train, which consists of 4 oscillation cycles, is observed only in pixel 4, located in the trailing spot. The duration of the wave train is approximately 2 hours, and the duration of oscillation cycles varies from 40 to 20 minutes. It should be noted that it is in pixel 4 that the greatest brightness temperature during the flare is observed. Possibly, weak QPOs can be distinguished in pixel 3, which is near pixel 4, and even weaker QPOs are in pixel 2, also located in the trailing spot of the AR but at a greater distance from pixel 4 than pixel 3.

Thus, in NOAA AR 11302, two hours before an M4.4 class flare, QPOs of microwave emission are observed, localized in the compact zone where the greatest brightness temperature during the flare was recorded.

3 Conclusions

Based on observations with the Nobeyama Radioheliograph we have analyzed the time profiles of brightness temperatures of microwave emission at a frequency of 17 GHz in two ARs (NOAA AR 11283 and 11302) before M5.3 and M4.4 flares, respectively. In both cases, the wave trains of preflare QPOs with low Q-factor (duration of 3–4 oscillation cycles) were observed. The QPOs of microwave emission are localized in compact zones coinciding with areas where the maximum brightness temperature was observed during the flares.

The work was carried out within the framework of the state assignment No. 1021032422589-5.

References

Abramov-Maximov V.E., Gelfreikh G.B., Shibasaki K., 2011. Solar Phys., vol. 273, pp. 403–412.

Abramov-Maximov V.E., Bakunina I.A., 2018. Phys. At. Nuclei, vol. 81, no. 3, pp. 379–383.

Abramov-Maximov V.E., Bakunina I.A., 2019. Geomagn. Aeron., vol. 59, no. 7, pp. 822–826.

Abramov-Maximov V.E., Bakunina I.A., 2020. Geomagn. Aeron., vol. 60, no. 7, pp. 846–852.

Avdyushin S.I., Bogomolov A.F., Borisova E.A., et al., 1985. Akademiia Nauk SSSR, Doklady, vol. 283, no. 1, pp. 67–70. (In Russ.)

Aver'yanikhina E., Paupere M., Ozolins G., Elias M., 1982. Issled. Solntsa i Krasnykh Zvezd., no. 16, pp. 61–74. (In Russ.)

Aleshin V.I., Kobrin M.M., Korshunov A.I., 1973. Radiophys. Quantum Electron., vol. 16, no. 5, pp. 571–576.

Arbuzov S.I., 1979. Radiophys. Quantum Electron., vol. 22, no. 10, pp. 803–811.

Berulis I.I., Molchanov A.P., Olyanyuk V.P., et al., 1973. Radiophys. Quantum Electron., vol. 16, no. 9, pp. 1047–1049.

Berulis I.I., Kozlovskii A.L., Losovskii B.Y., et al., 1983. Sov. Astron., vol. 27, no. 5, p. 563.

Bystrov M.V., Kobrin M.M., Snegirev S.D., 1978. Sov. Astron. Lett., vol. 4, pp. 76–77.

Bystrov M.V., Kobrin M.M., Snegirev S.D., 1979. Geomagn. Aeron., vol. 19, pp. 197–199.

Durasova M.S., Kobrin M.M., Yudin O.I., 1971. Nature, vol. 229, pp. 82–84.

Gelfreikh G.B., Grechnev V.V., Kosugi T., Shibasaki K., 1999. Solar Phys., vol. 185, pp. 177–191.

Gelfreikh G.B., Nagovitsyn Yu.A., Nagovitsyna E.Yu., 2006. Publ. Astron. Soc. Japan, vol. 58, pp. 29–35.

Kobrin M.M., Pakhomov V.V., Durasova M.S., et al., 1973a. Radiophys. Quantum Electron., vol. 16, pp. 1036–1039.

Kobrin M.M., Korshunov A.I., Snegirev S.D., Timofeev B.V., 1973b. Bull. Solnechnye Dannye, no. 10, p. 79–85. (In Russ.)

Kobrin M.M., Semenova S.V., Pahomov V.V., Pahomova O.A., Fridman V.M., 1981. Astron. Tsirk., no. 1201, p. 1.

Korshunov A.I., Prokof'eva N.A., 1976. Bull. Solnechnye Dannye, no. 2, pp. 52–56. (In Russ.)

Sych R., Nakariakov V.M., Karlicky M., Anfinogentov S., 2009. Astron. Astrophys., vol. 505, pp. 791–799.

Tan B., Yu Z., Huang J., Tan C., Zhang Y., 2016. Astrophys. J., vol. 833, id. 206.